The RNA m^{5}C Methylase NSUN2 Modulates Corneal Epithelial Wound Healing

Guangying Luo,[1,2] Weiwei Xu,[1,2] Xiaoyan Chen,[1,2] Wenji Xu,[1,2] Shuai Yang,[3] Jiao Wang,[1,2] Yong Lin,[1,2] Peter S. Reinach,[1,2] and Dongsheng Yan[1,2]

[1]School of Ophthalmology and Optometry, Eye Hospital, Wenzhou Medical University, Wenzhou, Zhejiang, China
[2]State Key Laboratory of Ophthalmology, Optometry and Visual Science, Wenzhou, Zhejiang, China
[3]Laboratory of RNA Epigenetics, Institutes of Biomedical Sciences, Fudan University, Shanghai, China

Correspondence: Dongsheng Yan, School of Ophthalmology and Optometry, Eye Hospital, Wenzhou Medical University, Wenzhou, Zhejiang, China; dnaprotein@hotmail.com or yandsh@eye.ac.cn.

Received: August 19, 2022
Accepted: February 8, 2023
Published: March 2, 2023

Citation: Luo G, Xu W, Chen X, et al. The RNA m^{5}C methylase NSUN2 modulates corneal epithelial wound healing. *Invest Ophthalmol Vis Sci.* 2023;64(3):5. https://doi.org/10.1167/iovs.64.3.5

Purpose. The emerging epitranscriptomics offers insights into the physiopathological roles of various RNA modifications. The RNA methylase NOP2/Sun domain family member 2 (NSUN2) catalyzes 5-methylcytosine (m^{5}C) modification of mRNAs. However, the role of NSUN2 in corneal epithelial wound healing (CEWH) remains unknown. Here we describe the functional mechanisms of NSUN2 in mediating CEWH.

Methods. RT-qPCR, Western blot, dot blot, and ELISA were used to determine the NSUN2 expression and overall RNA m^{5}C level during CEWH. NSUN2 silencing or overexpression was performed to explore its involvement in CEWH both in vivo and in vitro. Multi-omics was integrated to reveal the downstream target of NSUN2. MeRIP-qPCR, RIP-qPCR, and luciferase assay, as well as in vivo and in vitro functional assays, clarified the molecular mechanism of NSUN2 in CEWH.

Results. The NSUN2 expression and RNA m^{5}C level increased significantly during CEWH. NSUN2 knockdown significantly delayed CEWH in vivo and inhibited human corneal epithelial cells (HCEC) proliferation and migration in vitro, whereas NSUN2 overexpression prominently enhanced HCEC proliferation and migration. Mechanistically, we found that NSUN2 increased ubiquitin-like containing PHD and RING finger domains 1 (UHRF1) translation through the binding of RNA m^{5}C reader Aly/REF export factor. Accordingly, UHRF1 knockdown significantly delayed CEWH in vivo and inhibited HCEC proliferation and migration in vitro. Furthermore, UHRF1 overexpression effectively rescued the inhibitory effect of NSUN2 silencing on HCEC proliferation and migration.

Conclusions. NSUN2-mediated m^{5}C modification of *UHRF1* mRNA modulates CEWH. This finding highlights the critical importance of this novel epitranscriptomic mechanism in control of CEWH.

Keywords: NSUN2, RNA m^{5}C methylation, corneal epithelial wound healing

After tissue injury, a wound healing process is initiated that ultimately restores normal tissue function and structural integrity.[1] This response is an extremely complex process requiring interactions between different receptor-linked signaling pathways that control diverse gene expression events underlying recovery of homeostasis.[2] Defects in these processes can cause chronic wound disorders.[2] These aberrant responses include chronic increases in inflammation and tissue scarring as a consequence of fibrosis.[2] Hence, normal wound healing is an essential physiological response that restores innate function in tissues, such as the skin and other soft tissues.

The cornea consists of five well-differentiated tissue layers: the epithelium, Bowman's layer, the stroma, Descemet's membrane, and the endothelium.[3] Under normal conditions, the corneal epithelium continuously undergoes self-renewal, which is requisite for maintaining tissue integrity and transparency. After injury, it is imperative that the wound healing response is accelerated to decrease the likelihood of pathogenic infiltration into the stroma.[3] If clinical conditions such as diabetic corneas, persistent corneal epithelial defects, chemical corneal injury, and herpes simplex keratitis impair this process, restoration of visual competence can be severely compromised.[4–6] Currently, traditional treatment of this condition mainly includes lubricants, ointments, bandage lenses, amniotic membranes, autologous serum eye drops, and corneal transplants.[4] However, in recent years, experimental treatments increasingly focus on promoting corneal epithelial cell proliferation and migration or activating epithelial stem cell differentiation rather than on transient symptomatic relief alone, because we better understand the multifactorial mechanisms accelerating corneal epithelial wound healing (CEWH).[3,7–9] The most notable shift seems to be the application of growth factor in CEWH dysfunction, such as epidermal growth factor, insulin-like growth factor-1, nerve growth factor, and human growth hormone.[4] In particular, β-cellulin, an epidermal growth factor family member,

stimulates ERK1/2 phosphorylation for triggering recovery from corneal injury.[10] In addition, a report demonstrated that hyaluronan, a vital component of the corneal limbal stem cell niche, plays a significant role in maintaining the limbal stem cell phenotype.[11] The disruption of this specific hyaluronan leads to compromised corneal epithelial regeneration, opening possible new therapeutic avenues for treating limbal stem cell deficiency. Another important area of recent research relates to emerging microRNA therapy promoting corneal wound healing.[12] However, despite the increase in new potential treatments based on the physiological structure and molecular function of corneal epithelium, the specific mechanisms involved in CEWH remain poorly understood. Thus, clarifying the detailed mechanisms underlying corneal epithelial repair after an injury is vital for understanding the process driving wound healing.

Corneal epithelium, the eye's outermost layer, is particularly vulnerable to damage because it directly interacts with the external environment. This interaction is an essential factor that affects transcriptional and post-transcriptional control of gene expression levels that are determinants of RNA metabolism and protein synthesis and, in turn, the physiopathological phenotype.[13–15] This realization is highly suggestive of the role played by epigenetic regulation in controlling CEWH because epigenetics serves as an important bridge between environment and phenotypes. These bridge elements that provide epigenetic control mainly include DNA methylation, histone modification, and noncoding RNA, which elicit control of phenotypic expression via modulating gene expression patterns through regulating transcriptional and post-transcriptional events.[16] We have evaluated the time-dependent global DNA methylation changes and their regulatory mechanisms during CEWH.[17] Also, our recent study described in detail the role of histone methylase SUV39H1 in CEWH.[18] In addition, we elucidated the effects of marked declines in miR-204 and miR-184 expression levels in CEWH.[19,20] Collectively, epigenetic regulatory mechanisms have been well-established as crucial contributors to CEWH. Apart from traditional epigenetics, we have recently undertaken studies to characterize RNA modifications that are novel epitranscriptomics markers of functional mechanisms in CEWH.

RNA 5-methylcytosine (m^5C), an abundant modification in RNA, has been implicated in RNA metabolism by a growing number of studies.[21] The NOP2/Sun domain family member 2 (NSUN2) methylase catalyzes nearly the majority of reactions mediating mRNA m^5C formation.[22,23] Once RNA m^5C formation has occurred, it can be read by the nuclear reader protein Aly/REF export factor (ALYREF), which may control mRNA export and promote mRNA translation.[23] The cytoplasmic reader protein Y-box binding protein 1 (YBX1) recognizes RNA m^5C and regulates mRNA stability in an NSUN2-dependent mechanism.[24] NSUN2-mediated RNA m^5C has been linked to maternal-to-zygotic transition, adipogenesis, and carcinogenesis.[25–27] All these lines of emerging evidence have given rise to logical speculation that RNA m^5C modifications might act as a novel epigenetic marker with profound biological significance in CEWH.

Herein, using dot blot, RT-qPCR, and Western blot analysis, the results indicate that both RNA m^5C modifications and NSUN2 are significantly elevated in CEWH. We substantiate that NSUN2 is a CEWH contributor and clarify that NSUN2/RNA m^5C targeting ubiquitin-like containing PHD and RING finger domains 1 (UHRF1) modulates CEWH. Our findings shed light on the functional mechanisms of NSUN2 in CEWH, suggesting targeting RNA methylase as a potential therapeutic strategy for repairing damaged corneas.

Methods

Mice and CEWH Model

Eight-week-old C57BL/6 mice were obtained from the Vital River Laboratories (Beijing, China) and bred at the Wenzhou Medical University Experimental Animal Center. All animal experiments were performed in compliance with the ARVO Statement for the Use of Animals in Ophthalmic and Vision Research and approved by the Wenzhou Medical University Animal Care and Use Committee.

Mice were used for CEWH experiments based on previous well-established protocols.[17] Briefly, mice were anesthetized (13 mg/kg xylazine and 87 mg/kg ketamine). Next, a corneal rust ring remover (The Alger Company, Inc., Lago Vista, TX, USA) was used to debride the entire corneal epithelium of the right eyes labeled as wound healing (WH) groups, and the left eyes were untreated and labeled as normal control (CT) groups. After 48 hours, the corneal epithelium from these two groups was collected for molecular biological studies. Additionally, anesthetized mice were used for intrastromal small interfering RNA (siRNA) injection for silencing corneal epithelial genes in accordance with well-established protocols.[18] Briefly, polyethylenimine (PEI; Polyplus-transfection, New York, NY, USA)-complexed siRNA was injected into the anterior stroma. We assigned 100 µM siNSUN2 or siUHRF1 or siALYREF injected into the right eyes to either siNSUN2 or siUHRF1 or siALYREF groups, and the left eyes were injected with negative control (NC) and assigned to the NC groups. Six hours after intrastromal siRNA injection, the CEWH model was established by creating 2-mm-wide wounds in the right and left eyes. Fluorescein sodium-stained corneal wound areas were imaged with the slit-lamp microscope and quantified with the ImageJ software at 0 hour and 24 hours.

Cell Culture and Gene Manipulation

SV40-immortalized human corneal epithelial cells (HCECs) were donated by Araki Sasaki Kagoshima (Miyata Eye Clinic, Japan) and cultured in DMEM/F12 medium (Invitrogen, Carlsbad, CA, USA) supplemented with 10% fetal bovine serum (Invitrogen) in an incubator with 5% CO_2 and 37°C. No mycoplasma contamination was detected in the cultured HCECs. siRNA transfection was performed in HCECs for target gene silencing through treatment with lipofectamine RNAiMAX (Invitrogen). Lentivirus infection was performed in HCECs to generate target gene overexpression through HitransG A or HitransG P (Genechem Co., Ltd., Shanghai, China). Next, genetically manipulated HCECs were used for functional cell assays and molecular biological studies.

RT-qPCR

TRIzol reagent (Invitrogen) was utilized to isolate total RNA of mouse corneal epithelium or HCECs. RNA quality was assessed by NanoDrop One (Thermo Fisher Scientific, Waltham, MA, USA). RNAs were used for RT-qPCR based on previous well-established protocols.[17] Briefly, RNAs were reverse transcribed into cDNAs with random primer, and cDNAs were further amplified using specific primers (Supplementary Table S1). The target gene expression

was quantified with $2^{-\Delta\Delta Ct}$ method based on the β-actin normalized data.

Western Blot

Total protein of mouse corneal epithelium or HCECs was extracted using a RIPA lysis (Beyotime, Shanghai, China) and a SpectraMax M5 microplate reader (Molecular Devices, San Jose, CA, USA) was used to determine the protein concentration at 562 nm. Western blot analysis of proteins was performed based on previous well-established protocols.[17] Briefly, proteins were separated via sodium dodecyl sulfate polyacrylamide gel electrophoresis and transferred to a nitrocellulose membrane, followed by incubating with primary antibodies and then horseradish peroxidase-conjugated secondary antibodies. Next, the target protein bands were visualized and analyzed with AlphaView FluorChemQ (ProteinSimple, Santa Clara, CA).

Dot Blot

Total RNAs were further purified by RNase-free DNase I (Roche Diagnostics, Mannheim, Germany), phenol/chloroform extraction, and ethanol precipitation. Dot blot analysis was used to detect the RNA m^5C methylation level in the purified RNAs with well-established protocols.[28] Briefly, the denatured RNAs were spotted onto a nylon membrane (Thermo Fisher Scientific, 77016), followed by ultraviolet cross-linking, 5% fat-free milk blocking, and m^5C antibody (Diagenode, Denville, NJ; C15200081) and horseradish peroxidase-conjugated secondary antibodies (CST, 7076) incubating. The RNA m^5C dots were visualized and analyzed with AlphaView FluorChemQ (ProteinSimple).

RNA m^5C ELISA

For performing RNA m^5C ELISA, RNAs were bound to assay wells, followed by incubation with the m^5C fluorescence detection complex solution. Then the fluorescence was measured on a SpectraMax M5 microplate reader (Molecular Devices) at $530_{ex}/590_{em}$ nm. Finally, we utilized linear regression analysis to calculate the RNA m^5C methylation level.

EdU Assay

HCEC proliferation activity was assessed according to a well-established protocol.[18] Briefly, approximately 3000 HCECs were cultured in a 96-well plate (Corning, Corning, NY, USA). After 24 hours, the HCECs were transfected with siRNA or infected with a lentivirus. The HCEC proliferating activity was tested using a Click-iT EdU Alexa Fluor 594 Imaging Kit (Invitrogen, C10339). The fluorescein-stained HCECs were imaged with a microscope (Carl Zeiss Meditec, Jena, Germany), followed by using ImageJ software (National Institutes of Health, Bethesda, MD, USA) to quantify the proliferating cells.

Scratch Wound Assay

HCEC migratory activity was assessed according to a well-established protocol.[18] Briefly, 1.2×10^5 HCECs were cultured in 12-well plates (Corning). After 24 hours, HCECs were transfected with siRNA or infected with a lentivirus. Then a denuded lane of HCEC was created by scratching the surface with a 100-µL sterilized pipette tip. The time-dependent HCEC migratory activity was imaged with a microscope (Zeiss). ImageJ software (National Institutes of Health) was used to calculate the wound closure rate.

m^5C-RIP-qPCR

We used m^5C-RIP-qPCR to detect the m^5C level of the target gene based on a previous report with some modifications.[29] Briefly, the purified RNAs were incubated with the m^5C antibody (Diagenode) for immunoprecipitation. m^5C-modified RNAs were obtained by competitive elution with m^5C hydrochloride (Sigma-Aldrich). RT-qPCR was performed to test the enrichment of m^5C containing mRNA using $2^{-\Delta\Delta CT}$. IgG m^5C-RIP experiments were performed as a NC. Meanwhile, we also performed m^5C-RIP-qPCR using NC primer EEF1A1 (without RNA m^5C modification), which has been reported in previous studies.[23] The UHRF1 and EEF1A1 primer sequences for m^5C RIP-qPCR are listed in Supplementary Table S1.

RIP-qPCR

RIP-qPCR was used to detect the ALYREF enrichment on *UHRF1* mRNA in compliance with the instructions provided in the Magna RIP Kit (Merk Millipore, Burlington, MA, USA). Briefly, HCECs were lysed using a complete RIP lysis buffer. Next, Magnetic Beads Protein A/G conjugated with either the ALYREF antibody or IgG antibody were prepared for mixing with the RIP lysate. And pull-down RNA was digested with proteinase K buffer and purified with phenol: chloroform: isoamyl alcohol. RT-qPCR was used to analyze the retrieved RNA, and the UHRF1 primer sequences are listed in Supplementary Table S1. IgG RIP experiments were performed as a NC.

RNAm5Cfinder Prediction Analysis

RNAm5Cfinder is a tool for predicting RNA m^5C sites.[30] Briefly, the FASTA format *UHRF1* mRNA sequence was copied from the Nucleotide Database of NCBI. Then the sequence was put into the text area of the RNAm5Cfinder (http://www.rnanut.net/rnam5cfinder/). After submission, the software provides the predicted results.

Luciferase Activity Assay

The wild-type (WT) or mutant (MUT) UHRF1 CDS region was cloned into the pcDNA3.1(+)-hUHRF1(ns):3xGGGGS: Luciferase vector and generated the UHRF1-CDS WT and UHRF1-CDS MUT constructs, respectively. The UHRF1-CDS WT or the UHRF1-CDS MUT plasmids were cotransfected with siNSUN2 or NC into the HEK293 cells. After 48 hours transfection, the cells were lysed and the proteins were extracted. Luciferase activity was detected using Luciferase Assay System (Promega, Madison, WI, USA; E1500). The ratio of luciferase activity to the amount of luciferase protein produced was used to normalize the luciferase activity.

In Vivo Proliferation Assay

The anterior stroma of C57BL/6 mice was injected with PEI-complexed siRNA or NC. Then CEWH model was established by a corneal rust ring remover. After 48 hours, the eyeballs

Investigative Ophthalmology & Visual Science

were fixed with optimal cutting temperature compound (Thermo Fisher Scientific). Tissue sections were incubated with anti-Ki67 antibody (1:100; CST) overnight at 4°C following 4% paraformaldehyde fixing, 0.5% TritonX-100 permeabilization, and 5% goat serum blocking. These sections were further incubated with fluorescence-conjugated second antibodies, and the nucleus was stained with DAPI. Images were recorded with an inverted tiling microscope (DMi8, Leica, Wetzlar, Germany). The ratio of Ki67 positivity to the number of DAPI-positive nuclei was used to evaluate in vivo cell proliferation.

Statistical Analysis

All data in this study are expressed as the mean ± SEM. Statistical differences were performed by two-tailed Student's *t* test or two-way ANOVA, followed by asterisks denoting the level of significance (*$P < 0.05$, **$P < 0.01$, ***$P < 0.001$).

Results

Increased RNA m^{5}C Level and NSUN2 Expression in CEWH

To ascertain whether CEWH induces changes in the expression patterns of RNA m^{5}C modifications, we performed dot blot, RNA m^{5}C ELISA, RT-qPCR, and Western blot to evaluate RNA m^{5}C modification level and NSUN2 expression (CT vs. WH). Using this strategy, we found that RNA m^{5}C modification underwent significant upregulation during CEWH (Figs. 1A and B). RT-qPCR and Western blot verified that the gene and protein expression levels of NSUN2 in the WH group significantly increased as compared with the CT group (Figs. 2A–C). Furthermore, a four-pooled siRNA strategy was used to silence NSUN2 in HCECs, which decreased both NSUN2 protein and m^{5}C modification levels (Supplementary Fig. S1). Collectively, these data established that corneal epithelial injury-induced increases in NSUN2, which could be a novel molecular hallmark that may account for how the m^{5}C RNA methylation level increases during CEWH.

NSUN2 Modulates CEWH In Vivo and In Vitro

To explore the biological relevance of NSUN2 in vivo, we injected specific siRNA targeting NSUN2 into the anterior stroma of the corneas, which significantly decreased

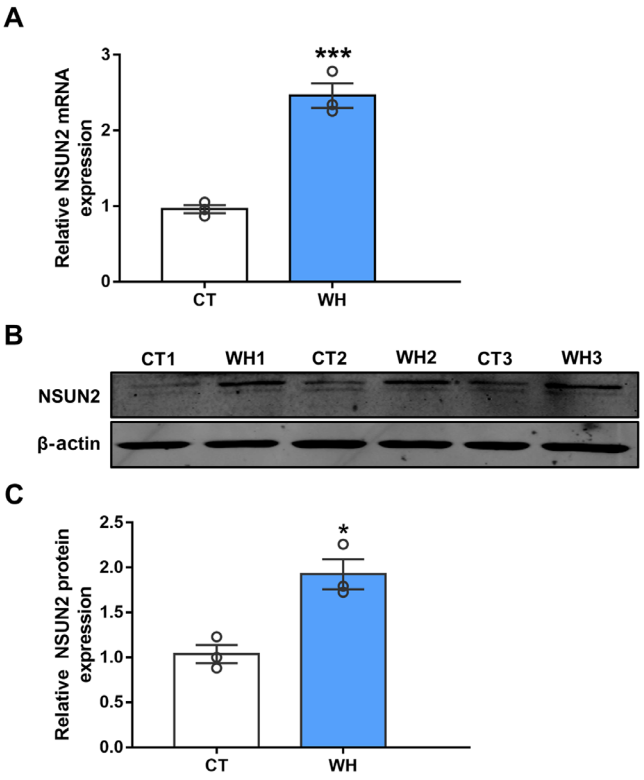

Figure 2. Increased NSUN2 mRNA and protein expression levels in CEWH. (**A**) RT-qPCR analysis of NSUN2 expression levels in CT and WH groups (2.46 ± 0.16-fold increase in WH group; n = 3/group; ***$P < 0.001$). (**B**) Western blots of CT and WH groups using NSUN2 and β-actin antibodies against the indicated proteins. (**C**) Densitometric analysis of the NSUN2 expression levels relative to the β-actin control level (1.92 ± 0.17 fold increase in WH group; n = 3/group; *$P < 0.05$). All data are shown as mean ± SEM.

the *NSUN2* mRNA expression level during CEWH (Fig. 3A), as well as the m^{5}C RNA methylation level (Fig. 3B). Compared with the NC-injected corneas, the unhealed areas in the siNSUN2-injected corneas were larger (Fig. 3C). Moreover, Ki67 staining revealed notable decreases in epithelial cell proliferation, when NSUN2 was silencing in the injured corneal epithelium (Supplementary Figs. S2A and B). These data suggest that silencing NSUN2 apparently delayed CEWH (Fig. 3D). This difference indicates an important role that NSUN2 plays in mediating CEWH. We next used HCECs

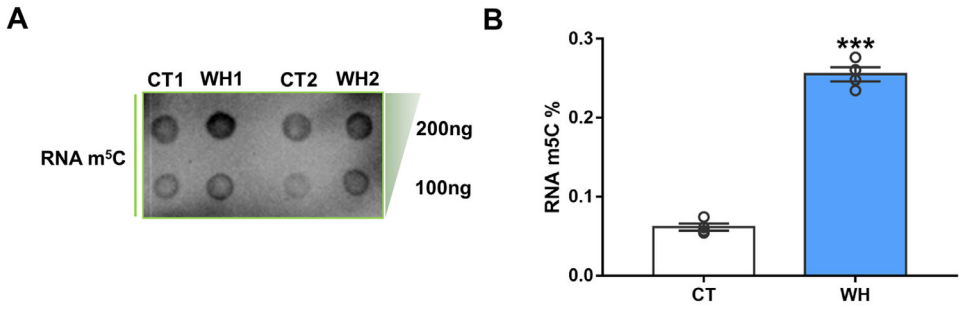

Figure 1. Increased RNA m^{5}C methylation level in CEWH. (**A**) Dot blots of CT and WH groups using m^{5}C antibody against the indicated RNA m^{5}C methylation. (**B**) ELISA analysis of the RNA m^{5}C methylation level (0.19% ± 0.01% increase in WH group; n = 4/group; ***$P < 0.001$). Corneal epithelial tissues from five mice were pooled for each set of RNA sample preparation and four independent sets of samples were established. All data are shown as mean ± SEM.

Investigative Ophthalmology & Visual Science

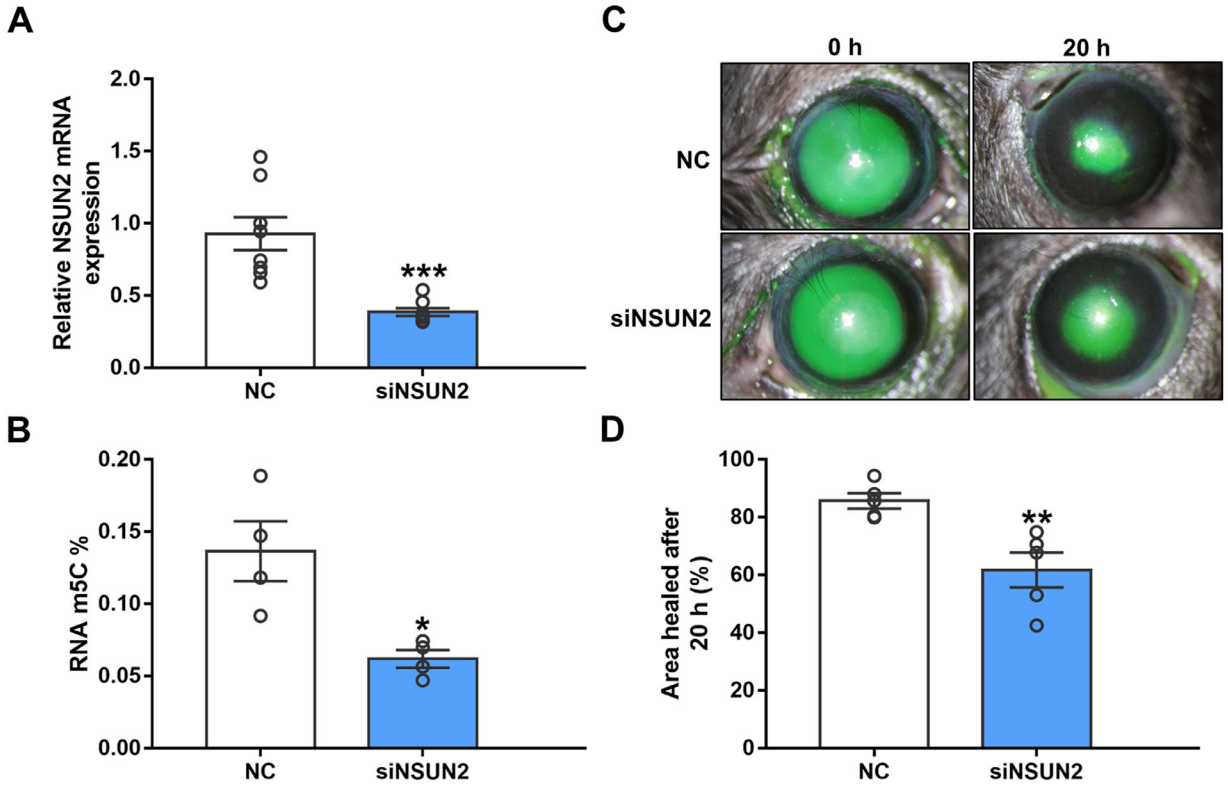

Figure 3. NSUN2-mediated RNA m^5C methylation regulates CEWH in vivo. (**A**) RT-qPCR analysis of NSUN2 expression level in response to NC or NSUN2 siRNA-mediated knockdown (0.38 ± 0.03-fold decrease in WH group; n = 8/group; ***$P < 0.001$). (**B**) RNA m^5C ELISA statistical analysis of NC and siNSUN2 groups (0.07% ± 0.02% decrease in siNSUN2 group; n = 4/group; *$P < 0.05$). Corneal epithelial tissues from five mice were pooled for each set of RNA sample preparation and four independent sets of samples were established. (**C**) Representative fluorescein-stained images of CEWH from NC and siNSUN2 groups at 0 hour and 20 hours. (**D**) Statistical analysis of the healed area at 20 hours in the NC group and after siNSUN2 treatment (23.94% ± 6.61% decrease in siNSUN2 group; n = 5/group; **$P < 0.01$). All data are shown as mean ± SEM.

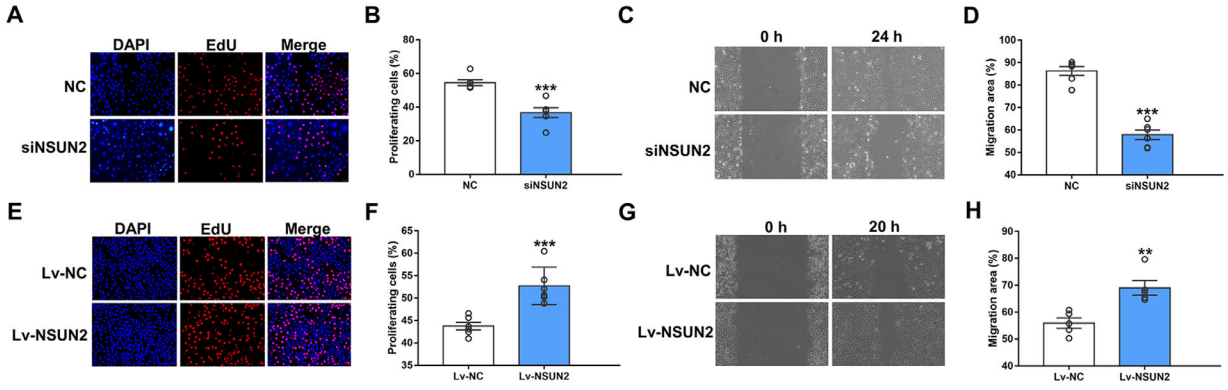

Figure 4. NSUN2 promotes cell proliferation and migration in vitro. (**A**) Immunofluorescence images of DAPI (*blue*) and EdU (*red*) in NC and siNSUN2-transfected HCECs. (**B**) Statistical analysis of proliferating cells in the NC and siNSUN2 groups (17.82% ± 3.38% decrease in siNSUN2 group; n = 6/group; ***$P < 0.001$). (**C**) Scratch wound images of the NC and siNSUN2-transfected HCECs at 0 hour and 24 hours. (**D**) Statistical analysis of migrating cells in the NC and siNSUN2 groups (28.45% ± 2.93% decrease in siNSUN2 group; n = 6/group; ***$P < 0.001$). (**E**) Immunofluorescence images of DAPI (*blue*) and EdU (*red*) in Lv-NC and Lv-NSUN2 infected HCECs. (**F**) Statistical analysis of proliferating cells in Lv-NC and Lv-NSUN2 groups (8.97% ± 1.91% increase in Lv-NSUN2 group; n = 6/group; ***$P < 0.001$). (**G**) Scratch wound images of Lv-NC and Lv-NSUN2 infected HCECs at 0 hour and 20 hours. (**H**) Statistical analysis of migrating cells in Lv-NC and Lv-NSUN2 groups (13.11% ± 3.33% increase in Lv-NSUN2 group; n = 5/group; **$P < 0.01$). All data are shown as mean ± SEM.

to clarify how silencing or overexpression of NSUN2 affects cell functions related to responses that underlie wound healing. In siNSUN2-transfected HCECs, the proliferation and migration activities were significantly inhibited, compared with the NC HCECs (Figs. 4A–D). In contrast, NSUN2 overexpression instead promoted the proliferation and migration of HCECs (Supplementary Fig. 3; Figs. 4E–H). Taken together, these results strongly indicate that there is a direct

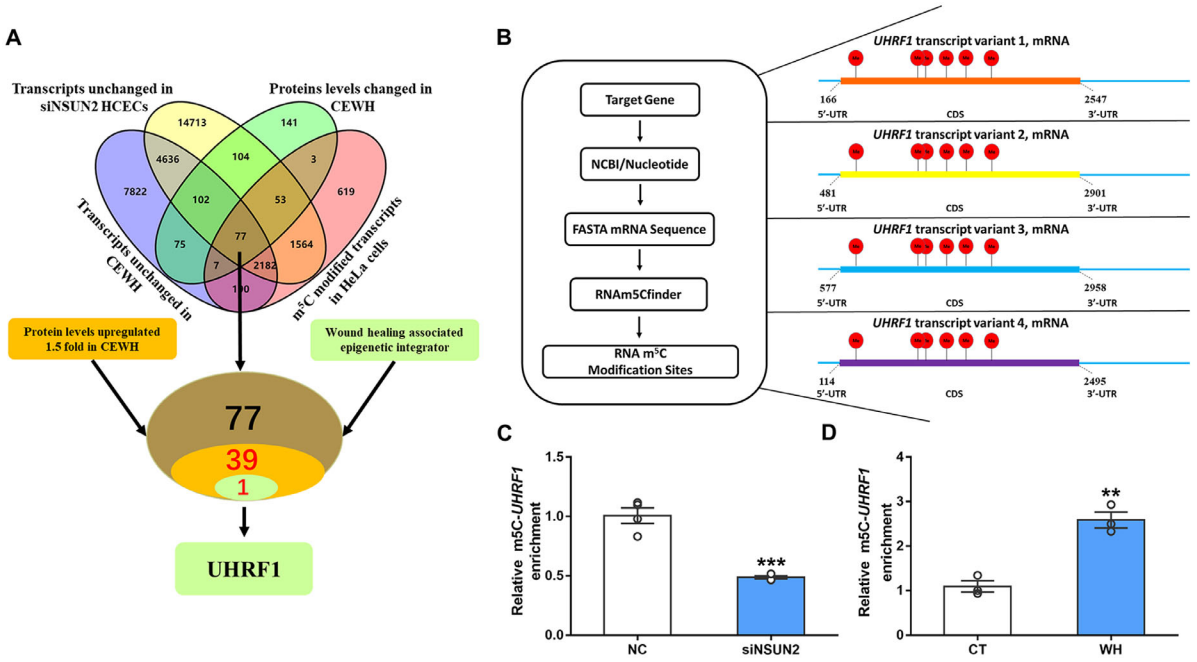

Figure 5. UHRF1 mRNA undergoes m^5C modification. (**A**) Multi-omics integration reveals UHRF1 in CEWH. (**B**) RNAm5Cfinder predicted m^5C modification sites of human *UHRF1* mRNA. (**C**) The abundance of methylated UHRF1 among RNA m^5C RIP-qPCR from NC and siNSUN2 transfected HCECs (0.49 ± 0.01 fold decrease in siNSUN2 group; n = 4/group; ***$P < 0.001$). (**D**) The abundance of methylated UHRF1 among RNA m^5C RIP-qPCR from CT and WH groups (2.59 ± 0.18-fold increase in WH group; n = 3/group; **$P < 0.01$). All data are shown as mean ± SEM.

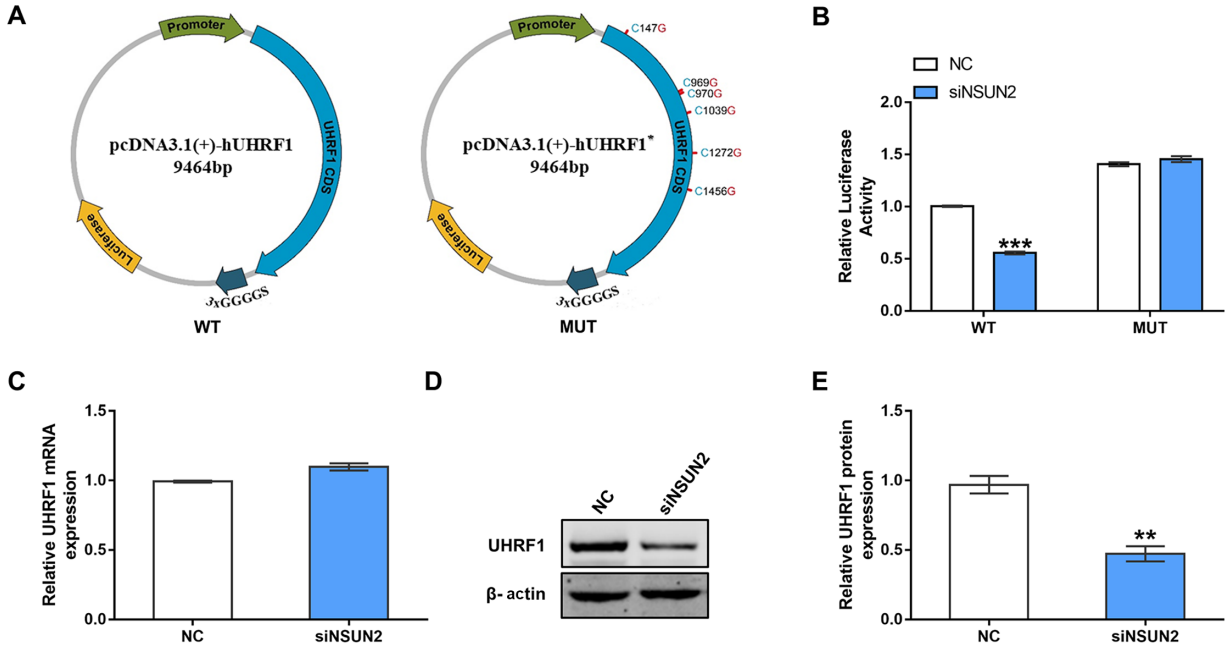

Figure 6. UHRF1 is the target of NSUN2 in HCECs. (**A**) WT UHRF1-CDS or MUT UHRF1-CDS sequence was fused with a firefly luciferase reporter. Schematic representation of MUT (147, 969, 970, 1039, 1272, and 1456 m^5C modification sites: C to G) CDS of pcDNA 3.1 vector to investigate the m^5C roles on UHRF1 expression. (**B**) Luciferase reporter assays measured the luciferase activities of UHRF1-CDS WT or UHRF1-CDS MUT in HEK293 cells with NSUN2 knockdown (0.56 ± 0.02 fold decrease in siNSUN2 group of WT; $n = 3$; ***$P < 0.001$). (**C**) RT-qPCR analysis of *UHRF1* mRNA expression levels in NC or siNSUN2-transfected HCECs. (**D**) Western blot analysis of NC and siNSUN2 groups using UHRF1 and β-actin antibodies against the indicated proteins. (**E**) Densitometric analysis of the UHRF1 expression levels relative to the β-actin control level (0.47 ± 0.05-fold decrease in siNSUN2 group; n = 3/group; **$P < 0.01$). All data are shown as mean ± SEM.

Investigative Ophthalmology & Visual Science

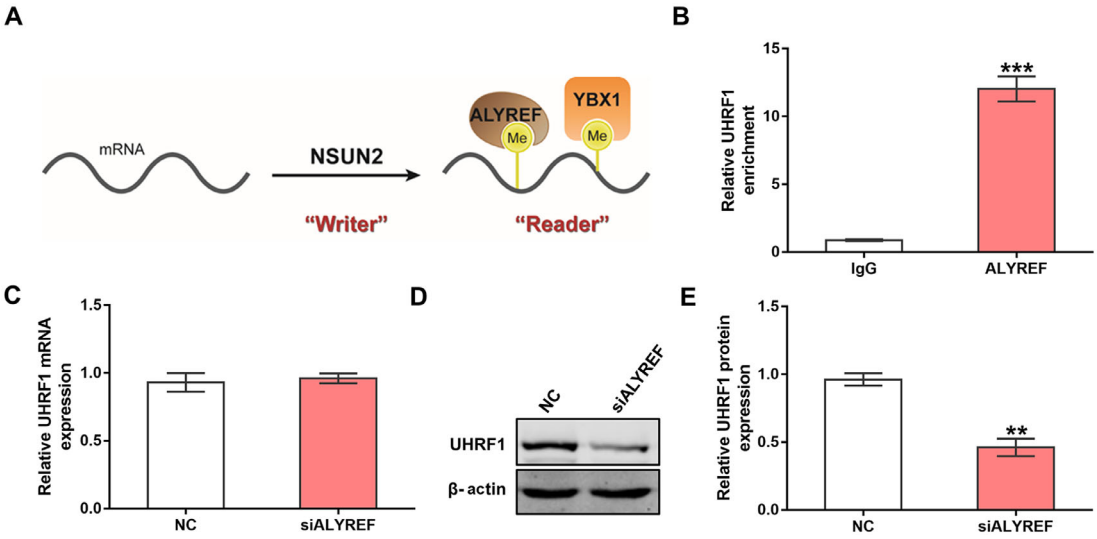

Figure 7. RNA m^{5}C reader ALYREF regulates UHRF1 translation. (**A**) Schematic diagram of RNA m^{5}C methylation "writer" and "readers." (**B**) RIP-qPCR analysis revealed that ALYREF enriched UHRF1 transcripts in HCECs (12.03 ± 0.93-fold increase in ALYREF group; n = 3/group; ***P < 0.001). (**C**) RT-qPCR analysis of *UHRF1* expression levels after treatment of HCECs with NC or siALYREF. (**D**) Western blot analysis of the NC and siALYREF groups using UHRF1 and β-actin antibodies against the indicated proteins. (**E**) Densitometric analysis of the UHRF1 expression levels relative to the β-actin control level (0.46 ± 0.06-fold decrease in siALYREF group; n = 3/group; **P < 0.01). All data are shown as mean ± SEM.

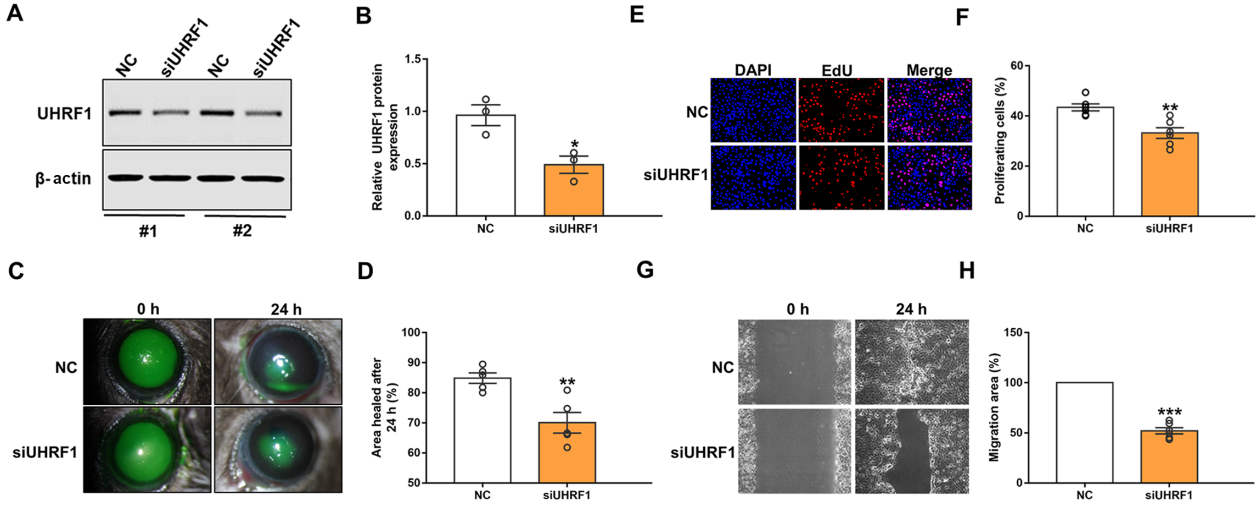

Figure 8. UHRF1 regulates CEWH in vivo and in vitro. (**A**) Western blot analysis of NC and siUHRF1 groups using UHRF1 and β-actin antibodies against the indicated proteins. (**B**) Densitometric analysis of the UHRF1 expression relative to the β-actin control (0.49 ± 0.08-fold decrease in siUHRF1 group; n = 3/group; *P < 0.05). (**C**) Representative fluorescein-stained images of CEWH from NC and siUHRF1 groups at 0 hour and 24 hours. (**D**) Statistical analysis of the healed area at 24 hours of the NC and after siUHRF1 treatment (14.84% ± 3.83% decrease in siUHRF1 group; n = 5/group; **P < 0.01). (**E**) Immunofluorescence images of DAPI (*blue*) and EdU (*red*) in NC and siUHRF1-transfected HCECs. (**F**) Statistical analysis of proliferating cells in the NC and siUHRF1-transfected HCECs (10.2% ± 2.53% decrease in siUHRF1 group; n = 6/group; **P < 0.01). (**G**) Scratch wound images of the NC and siUHRF1-transfected HCECs at 0 hour and 24 hours. (**H**) Statistical analysis of migrating cells in the NC and siUHRF1-transfected HCECs (47.88% ± 3.11% decrease in siUHRF1 group; n = 6/group; ***P < 0.001). All data are shown as mean ± SEM.

relationship between changes in NSUN2 expression levels and CEWH.

UHRF1 Is the RNA m^{5}C Modification Target of NSUN2

To clarify how NSUN2 modulates CEWH, we previously performed gene microarray and iTRAQ analyses to detect molecular expression changes underlying CEWH. RNA sequencing was also adopted to determine the effects of NSUN2 knockdown on RNA expression levels. The research strategy for filtering the target molecule *UHRF1* can be divided into three steps. First, we combined microarray, iTRAQ, and RNA sequencing data with m^{5}C-RIP-Seq data from Yang et al. to obtain an intersection and identified 77 molecules that might be regulated by NSUN2 (Fig. 5A; Supplementary Table S2). Second, based on experimental

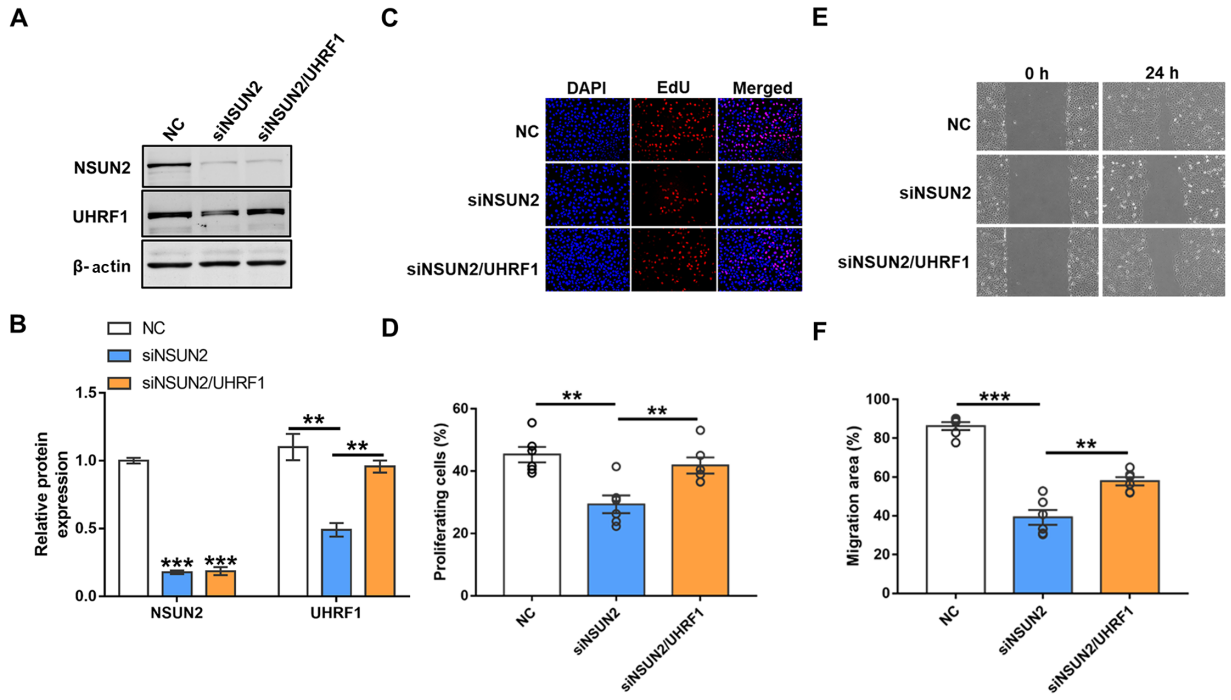

Figure 9. Overexpression of UHRF1 ameliorates the suppressive effects of NSUN2 silencing on HCEC proliferation and migration. (**A**) Western blot exhibited the protein level of NSUN2 and UHRF1 in NSUN2-silenced HCECs upon overexpression of UHRF1. (**B**) Densitometric analysis of the NSUN2 and UHRF1 expression relative to the β-actin control (for NSUN2, 0.18 ± 0.02-fold decrease in siNSUN2 group compared with NC group and a 0.19 ± 0.04-fold decrease in siNSUN2/UHRF1 group compared with NC group; for UHRF1, 0.49 ± 0.01-fold decrease in siNSUN2 group compared with NC group and 2.00 ± 0.09-fold increase in siNSUN2/UHRF1 group compared with siNSUN2 group; n = 3/group; ***$P < 0.001$; **$P < 0.01$). (**C**) EdU assays were adopted to assess the proliferative abilities of NSUN2-silenced HCECs upon overexpression of UHRF1. (**D**) Statistical analysis of proliferating cells in the NC, siNSUN2, and siNSUN2/UHRF1 groups (15.93% ± 3.77% decrease in siNSUN2 group compared with NC group and 12.43% ± 3.85% increase in siNSUN2/UHRF1 group compared with siNSUN2 group; n = 6/group; **$P < 0.01$). (**E**) Scratch wound assays were employed to evaluate the migratory abilities in NSUN2 silenced HCECs upon overexpression of UHRF1. (**F**) Statistical analysis of migrating cells in the NC, siNSUN2, and siNSUN2/UHRF1 groups (47.08% ± 4.26% decrease in siNSUN2 group compared with NC group and 18.62% ± 4.32% increase in siNSUN2/UHRF1 group compared with siNSUN2 group; n = 6/group; **$P < 0.01$; ***$P < 0.001$). All data are shown as mean ± SEM.

studies from our team and others,[26,31,32] we know that NSUN2-mediated RNA m^5C hypermethylation can promote mRNA translation. Therefore, we further filtered 39 upregulated molecules from the 77 molecules using proteomics data from CEWH, as NSUN2/RNA m^5C levels were significantly increased in CEWH. Proteins whose expression levels rose by at least 1.5-fold were classified as upregulated (Fig. 5A; Supplementary Table S2). Finally, we found that *UHRF1* was the most interesting molecule among the 39 identified molecules. This is because *UHRF1* is not only an oncogene but also an important epigenetic integrator that maintains DNA methylation and H3K9 methylation,[33] which has been reported to be involved in CEWH (Fig. 5A; Supplementary Table S2).[17,18] In addition, RNAm5Cfinder prediction analyses found that there are six RNA m^5C modification sites in human *UHRF1* transcript (Fig. 5B). Meanwhile, RNAm5Cfinder prediction analyses found that there are six higher confident RNA m^5C modification sites in mouse *Uhrf1* transcript (Supplementary Fig. S4). Importantly, m^5C-RIP-qPCR further showed that a significant reduction in the *UHRF1* mRNAs enrichment by the m^5C-specific antibody was detected in the siNSUN2 groups (Fig. 5C). Likewise, m^5C-RIP-qPCR also showed that a significant increase in the *Uhrf1* mRNAs enrichment by the m^5C-specific antibody was detected in the WH groups (Fig. 5D). In addition, we also evaluated m^5C enrichment using IgG or negative primers and found extremely low-enriched m^5C in siNSUN2 treated HCECs group or WH group (Supplementary Figs. S5A–D). In particular, the luciferase activity was significantly abated in UHRF1-WT when NSUN2 was silenced, whereas that of UHRF1-MUT was unaffected (Figs. 6A, 6B). Furthermore, we noticed that silencing NSUN2 barely changed the *UHRF1* mRNA expression level, although it decreased the UHRF1 protein expression level (Figs. 6C–E), supporting that NSUN2 regulates the translation of UHRF1. These data indicate that UHRF1 is a direct target of NSUN2.

RNA m^5C Reader ALYREF Facilitates UHRF1 mRNA Translation

Previous studies have demonstrated that m^5C methylated mRNA could be recognized directly by ALYREF and YBX1 (Fig. 7A).[23] YBX1 binding has been reported to promote mRNA degradation.[25] However, we have found that NSUN2 regulates the translation of UHRF1. More important, ALYREF protein level was significantly increased during CEWH, but YBX1 has no significant changes (Supplementary Figs. S6A, S6B). Hence, we next investigated whether

ALYREF is involved in the regulation of UHRF1 expression. RIP-qPCR revealed more enrichment of *UHRF1* mRNA in ALYREF pull-down compared with IgG pull-down (Fig. 7B). Moreover, silencing ALYREF barely changed the *UHRF1* mRNA expression level, although it decreased the UHRF1 protein expression level (Supplementary Figs. S7A–C; Figs. 7C–E). These results established that ALYREF could bind directly to UHRF1 mRNA and regulate its translation. In addition, we evaluated the effects of ALYREF knockdown on in vivo wound healing and in vitro cellular functions. As expected, silencing ALYREF apparently delayed CEWH in vivo (Supplementary Figs. S8A–D) and inhibited the proliferation and migration of HCECs (Supplementary Figs. S9A–D). Collectively, ALYREF regulates CEWH, possibly via augmenting UHRF1 translation.

UHRF1 Promotes CEWH

Because the functions of UHRF1 in CEWH remain unclear, we examined the expression level of UHRF1 in CEWH and found that the UHRF1 protein levels significantly increased in the WH group as compared with the CT group (Supplementary Figs. S10A and 10B). To further characterize the function of UHRF1 in CEWH, we first injected siUHRF1 into the anterior stroma of the corneas, which induced a significant decrease in the UHRF1 protein expression level during CEWH (Figs. 8A and B). Compared with NC-injected corneas, there was a larger unhealed area in siUHRF1-injected corneas (Fig. 8C). Moreover, Ki67 staining revealed notable decreases in epithelial cell proliferation when UHRF1 was silencing in the injured corneal epithelium (Supplementary Figs. S11A and 11B). These data indicate that UHRF1 silencing delayed CEWH (Fig. 8D). These results suggest an important role of UHRF1 in regulating CEWH. We next used HCECs to study how silencing of UHRF1 affects functions underlying wound healing. In siUHRF1-transfected HCECs, the proliferation and migration were inhibited significantly compared with NC HCECs (Figs. 8E–H). Moreover, we showed that UHRF1 overexpression partially rescued decreases in cell proliferation and migration activity resulting from NSUN2 silencing in HCECs (Figs. 9A–F). Collectively, these results indicated that UHRF1 is critical for NSUN2 to modulate CEWH.

Discussion

Studies using the corneal epithelium to characterize the events underlying wound healing provides an advantageous model system to clarify the involvement of epigenetics in mediating the control of tissue renewal. This approach provides insight into how epigenetic factors regulate healing through modulating CEWH. First, injury initiates corneal epithelial regeneration over the denuded surface, which requires continuous increases in both RNA metabolism and persistent protein synthesis.[3,7,34] Although genetic mutations have not yet been found in the CEWH, we and others identified DNA methylation, histone modification, and microRNA involvement in this process.[17–20,35] Second, the corneal epithelium constantly undergoes self-renewal to maintain its structural continuity because its constituents have a finite lifetime.[7] The ability of CEWH renders it vulnerable to evolutionary pressures that seek selective advantages that are able to adapt to environmental pressures that otherwise challenge its longevity.[7] Therefore, suppose a given RNA modification confers a selective advantage, such as enhanced mRNA degradation and translation.[31] It is likely that corneal epithelial injury–response mRNAs should have evolved to require high-level mRNA modifications that maximize this advantage for the corneal epithelial renewal process.

The addition of mRNA m^5C modifications to RNA is mediated by m^5C methylases (NSUN2).[36] In this study, we found that the RNA m^5C modification level is significantly upregulated in CEWH. Furthermore, NSUN2 expression is also significantly increased in CEWH. Clearly, these increases are unlikely to occur by chance. Previous studies linking NSUN2 to epithelial cell proliferation and migration led us to ask if upregulated NSUN2 underlies augmentation of the CEWH response, leading to wound closure.[37] Here, we report that engineering losses in NSUN2 function significantly delayed the CEWH in vivo and inhibited HCEC proliferation and migration in vitro. In contrast, engineering gain of NSUN2 function distinctly promoted both HCEC proliferation and migration in vitro. These findings suggest that NSUN2 upregulation might hasten wound closure by stimulating the CEWH response. Additionally, we inferred that NSUN2 is also involved in regulating of repair processes of other injured tissues since the NSUN2/RNA m^5C expression pattern is widely distributed in diverse mammalian tissues.[23,38,39] More generally, this study implies that engineering RNA methylase upregulation may improve tissue injury repair.

It is surprising that NSUN2 can modulate CEWH through mechanisms that depend on RNA m^5C-modified *UHRF1*

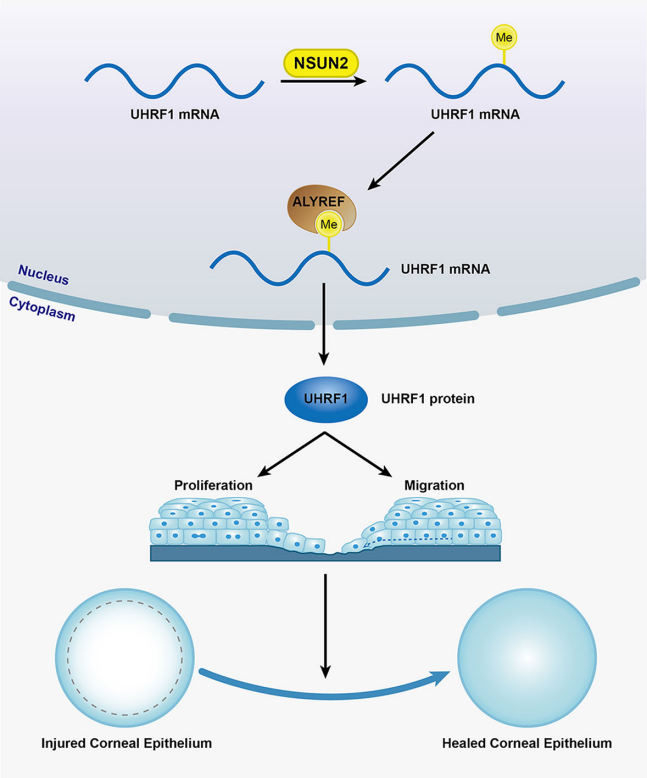

Figure 10. Schematic model of a potential regulatory mechanism by which NSUN2-mediated RNA m^5C methylation modulates CEWH. NSUN2 mainly facilitates UHRF1 translation through the recruitment of the RNA m^5C reader, ALYREF.

mRNA translation. Our results were also supported by the presence of RNA m^5C modification sites in UHRF1 transcripts from recent studies based on the epitranscriptome profile of RNA m^5C.[40–42] UHRF1 is a well-known oncogene in various types of cancers that possesses a series of phenotypes resembling those in cells undergoing proliferation and migration during CEWH.[43,44] There is no doubt that UHRF1 is a regulator of CEWH since engineering losses in UHRF1 function significantly delayed CEWH in vivo, and inhibited HCEC proliferation and migration in vitro. Interestingly, UHRF1 is emerging as an epigenetic integrator that maintains the DNA methylation level and histone modification pattern to control cell phenotype.[45] Most notably, we have demonstrated previously that the DNA methylation level and histone modification pattern are underlying mechanisms in CEWH.[17,18] This realization first shows that UHRF1 is an epigenetic cross-talk hub connecting RNA m^5C modification to DNA methylation and histone modification. Overall, this conclusion from the well-recognized CEWH model is a theoretical epigenetics innovation; our findings not only provide novel insights on CEWH, but also highlight their applicability for RNA m^5C-targeted therapy in a variety of wound healing-associated phenotypes.

It is generally well-accepted that ALYREF acts as an RNA m^5C reader and ALYREF functions via recognition and affects the translation of RNA m^5C methylated transcripts.[23,26] Therefore, we performed a preliminary analysis of the ALYREF binding capacity to *UHRF1* mRNA and the effects of engineering loss of ALYREF function on UHRF1 expression. The results prompt us to propose a potential NSUN2/m^5C-dependent model whereby ALYREF activates UHRF1 during CEWH. Further detailed mechanistic studies are warranted to focus on RNA m^5C-modified UHRF1 mRNA targeted by ALYREF in regulating CEWH.

In this study, we found RNA m^5C methylase NSUN2 promotes CEWH, which could also have implications for diabetic corneas, persistent corneal epithelial defects, chemical corneal injury, and herpes simplex keratitis. Individuals with any of these ocular surface disorders most commonly have delayed corneal epithelium healing. Therefore, how to engineer NSUN2/RNA m5C level to improve cornea injury repair has become an exciting issue. The first option is the adeno-associated virus–mediated gene therapy for corneal epithelial injury since viral-mediated gene therapy has been successfully applied to deliver specific genes into the cornea for overexpression of target genes,[46] which indicates that adeno-associated virus–mediated gene therapy is a promising strategy that involves the delivery of genetic material to corneal epithelium through augmenting NSUN2 expression. Furthermore, developing small molecules to induce NSUN2 expression or to increase m^5C modification levels is another potential strategy. We also note that genome editing technology has emerged as a practical treatment option for ocular diseases.[47] Most strikingly, gene editing via mRNA-based CRISPR delivery successfully suppresses herpes simplex keratitis in corneas.[48] This advancement raises the possibility that a CRISPR system may have a role in engineering NSUN2/RNA m^5C in the corneal epithelium. Moreover, recent studies established that either a CRISPR-Cas13 or CRISPR-Cas9 fusion m^6A methylase can specifically mediate efficient m^6A installation into mRNA transcripts.[49,50] These findings constitute a crucial step toward engineering precision epitranscriptomics. Although, at present, there are scant reports showing that a programmable RNA m^5C modification directed at NSUN2 can be inserted with a CRISPR-Cas system, this epitranscriptomic editing strategy has the potential to fulfill this objective.

Collectively, we propose a preliminary working model in which the NSUN2/ALYREF/m^5C-UHRF1 signaling axis is an essential mechanism that modulates CEWH (Fig. 10). Clearly, injury repair is present in many mammalian tissues, and the elucidation of analogous mechanisms should be relevant to the occurrence and therapy of a variety of wound healing-associated phenotypes.

Acknowledgments

The authors thank Araki Sasaki Kagoshima (Miyata Eye Clinic, Kagoshima, Japan) for the kind gift of the HCEC cell line.

Supported, in part, by the National Natural Science Foundation of China (81700801 and 81900818), Zhejiang Provincial Natural Science Foundation of China (LY21H120005 and LZ23H160002), Foundation of Wenzhou Science & Technology Bureau (H20220009), 973 Project (2012CB722303) from the Ministry of Science and Technology of China, Science Foundation of Wenzhou Medical University (QTJ11020).

Disclosure: **G. Luo,** None; **W. Xu,** None; **X. Chen,** None; **W. Xu,** None; **S. Yang,** None; **J. Wang,** None; **Y. Lin,** None; **P.S. Reinach,** None; **D. Yan,** None

References

1. Eming SA, Wynn TA, Martin P. Inflammation and metabolism in tissue repair and regeneration. *Science*. 2017;356:1026–1030.
2. Gurtner GC, Werner S, Barrandon Y, Longaker MT. Wound repair and regeneration. *Nature*. 2008;453:314–321.
3. Ljubimov AV, Saghizadeh M. Progress in corneal wound healing. *Prog Retin Eye Res*. 2015;49:17–45.
4. Wirostko B, Rafii M, Sullivan DA, Morelli J, Ding J. Novel therapy to treat corneal epithelial defects: a hypothesis with growth hormone. *Ocul Surf*. 2015;13:204–212.e201.
5. Iyer G, Srinivasan B, Agarwal S. Algorithmic approach to management of acute ocular chemical injuries-I's and E's of management. *Ocul Surf*. 2019;17:179–185.
6. Koujah L, Allaham M, Patil CD, et al. Entry receptor bias in evolutionarily distant HSV-1 clinical strains drives divergent ocular and nervous system pathologies. *Ocul Surf*. 2021;21:238–249.
7. Liu CY, Kao WW. Corneal epithelial wound healing. *Prog Mol Biol Transl Sci*. 2015;134:61–71.
8. Lavker RM, Kaplan N, Wang J, Peng H. Corneal epithelial biology: lessons stemming from old to new. *Exp Eye Res*. 2020;198:108094.
9. Barrientez B, Nicholas SE, Whelchel A, Sharif R, Hjortdal J, Karamichos D. Corneal injury: clinical and molecular aspects. *Exp Eye Res*. 2019;186:107709.
10. Jeong WY, Yoo HY, Kim CW. Beta-cellulin promotes the proliferation of corneal epithelial stem cells through the phosphorylation of erk1/2. *Biochem Biophys Res Commun*. 2018;496:359–366.
11. Gesteira TF, Sun M, Coulson-Thomas YM, et al. Hyaluronan rich microenvironment in the limbal stem cell niche regulates limbal stem cell differentiation. *Invest Ophthalmol Vis Sci*. 2017;58:4407–4421.
12. Rassi DM, De Paiva CS, Dias LC, et al. Review: microRNAS in ocular surface and dry eye diseases. *Ocul Surf*. 2017;15:660–669.
13. Takacs L, Toth E, Berta A, Vereb G. Stem cells of the adult cornea: from cytometric markers to therapeutic applications. *Cytometry A*. 2009;75:54–66.

14. Cavalli G, Heard E. Advances in epigenetics link genetics to the environment and disease. *Nature*. 2019;571:489–499.
15. Cayir A, Byun HM, Barrow TM. Environmental epitranscriptomics. *Environ Res*. 2020;189:109885.
16. Kan RL, Chen J, Sallam T. Crosstalk between epitranscriptomic and epigenetic mechanisms in gene regulation. *Trends Genet*. 2022;38:182–193.
17. Luo G, Jing X, Yang S, et al. DNA methylation regulates corneal epithelial wound healing by targeting miR-200a and CDKN2B. *Invest Ophthalmol Vis Sci*. 2019;60:650–660.
18. Yang S, Chen W, Jin S, et al. SUV39H1 regulates corneal epithelial wound healing via H3K9me3-mediated repression of p27. *Eye Vis (Lond)*. 2022;9:4.
19. An J, Chen X, Chen W, et al. MicroRNA expression profile and the role of miR-204 in corneal wound healing. *Invest Ophthalmol Vis Sci*. 2015;56:3673–3683.
20. Cao Q, Xu W, Chen W, et al. MicroRNA-184 negatively regulates corneal epithelial wound healing via targeting CDC25A, CARM1, and LASP1. *Eye Vis (Lond)*. 2020;7:35.
21. Squires JE, Patel HR, Nousch M, et al. Widespread occurrence of 5-methylcytosine in human coding and non-coding RNA. *Nucleic Acids Res*. 2012;40:5023–5033.
22. Khoddami V, Cairns BR. Identification of direct targets and modified bases of RNA cytosine methyltransferases. *Nat Biotechnol*. 2013;31:458–464.
23. Yang X, Yang Y, Sun BF, et al. 5-Methylcytosine promotes mRNA export - NSUN2 as the methyltransferase and ALYREF as an m(5)C reader. *Cell Res*. 2017;27:606–625.
24. Chen X, Li A, Sun BF, et al. 5-methylcytosine promotes pathogenesis of bladder cancer through stabilizing mRNAs. *Nat Cell Biol*. 2019;21:978–990.
25. Yang Y, Wang L, Han X, et al. RNA 5-methylcytosine facilitates the maternal-to-zygotic transition by preventing maternal mRNA decay. *Mol Cell*. 2019;75:1188–1202.e1111.
26. Liu Y, Zhao Y, Wu R, et al. mRNA m5C controls adipogenesis by promoting CDKN1A mRNA export and translation. *RNA Biol*. 2021;18:711–721.
27. Chellamuthu A, Gray SG. The RNA methyltransferase NSUN2 and its potential roles in cancer. *Cells*. 2020;9:1758.
28. Luo G, Xu W, Zhao Y, et al. RNA m(6) A methylation regulates uveal melanoma cell proliferation, migration, and invasion by targeting c-Met. *J Cell Physiol*. 2020;235:7107–7119.
29. Dominissini D, Moshitch-Moshkovitz S, Schwartz S, et al. Topology of the human and mouse m6A RNA methylomes revealed by m6A-seq. *Nature*. 2012;485:201–206.
30. Li J, Huang Y, Yang X, Zhou Y, Zhou Y. RNAm5Cfinder: a web-server for predicting RNA 5-methylcytosine (m5C) sites based on random Forest. *Sci Rep*. 2018;8:17299.
31. Courtney DG, Tsai K, Bogerd HP, et al. Epitranscriptomic addition of m(5)C to HIV-1 transcripts regulates viral gene expression. *Cell Host Microbe*. 2019;26:217–227.e216.
32. Li Q, Li X, Tang H, et al. NSUN2-mediated m5C methylation and METTL3/METTL14-mediated m6A methylation cooperatively enhance p21 translation. *J Cell Biochem*. 2017;118:2587–2598.
33. Ashraf W, Ibrahim A, Alhosin M, et al. The epigenetic integrator UHRF1: on the road to become a universal biomarker for cancer. *Oncotarget*. 2017;8:51946–51962.
34. Suzuki K, Saito J, Yanai R, et al. Cell-matrix and cell-cell interactions during corneal epithelial wound healing. *Prog Retin Eye Res*. 2003;22:113–133.
35. Lee SK, Teng Y, Wong HK, et al. MicroRNA-145 regulates human corneal epithelial differentiation. *PLoS One*. 2011;6:e21249.
36. Frye M, Harada BT, Behm M, He C. RNA modifications modulate gene expression during development. *Science*. 2018;361:1346–1349.
37. Frye M, Watt FM. The RNA methyltransferase Misu (NSun2) mediates Myc-induced proliferation and is upregulated in tumors. *Curr Biol*. 2006;16:971–981.
38. Huang T, Chen W, Liu J, Gu N, Zhang R. Genome-wide identification of mRNA 5-methylcytosine in mammals. *Nat Struct Mol Biol*. 2019;26:380–388.
39. Blanco S, Kurowski A, Nichols J, Watt FM, Benitah SA, Frye M. The RNA-methyltransferase Misu (NSun2) poises epidermal stem cells to differentiate. *PLoS Genet*. 2011;7:e1002403.
40. Liu J, Huang T, Chen W, et al. Developmental mRNA m(5)C landscape and regulatory innovations of massive m(5)C modification of maternal mRNAs in animals. *Nat Commun*. 2022;13:2484.
41. Wei Z, Panneerdoss S, Timilsina S, et al. Topological characterization of human and mouse m(5)C epitranscriptome revealed by bisulfite sequencing. *Int J Genomics*. 2018;2018:1351964.
42. He Z, Xu J, Shi H, Wu S. m5CRegpred: epitranscriptome target prediction of 5-methylcytosine (m5C) regulators based on sequencing features. *Genes (Basel)*. 2022;13:1326.
43. Xiang H, Yuan L, Gao X, et al. UHRF1 is required for basal stem cell proliferation in response to airway injury. *Cell Discov*. 2017;3:17019.
44. Jenkins Y, Markovtsov V, Lang W, et al. Critical role of the ubiquitin ligase activity of UHRF1, a nuclear RING finger protein, in tumor cell growth. *Mol Biol Cell*. 2005;16:5621–5629.
45. Rottach A, Frauer C, Pichler G, Bonapace IM, Spada F, Leonhardt H. The multi-domain protein Np95 connects DNA methylation and histone modification. *Nucleic Acids Res*. 2010;38:1796–1804.
46. Bastola P, Song L, Gilger BC, Hirsch ML. Adeno-associated virus mediated gene therapy for corneal diseases. *Pharmaceutics*. 2020;12:767.
47. Yu W, Wu Z. Ocular delivery of CRISPR/Cas genome editing components for treatment of eye diseases. *Adv Drug Deliv Rev*. 2021;168:181–195.
48. Yin D, Ling S, Wang D, et al. Targeting herpes simplex virus with CRISPR-Cas9 cures herpetic stromal keratitis in mice. *Nat Biotechnol*. 2021;39:567–577.
49. Wilson C, Chen PJ, Miao Z, Liu DR. Programmable m(6)A modification of cellular RNAs with a Cas13-directed methyltransferase. *Nat Biotechnol*. 2020;38:1431–1440.
50. Liu XM, Zhou J, Mao Y, Ji Q, Qian SB. Programmable RNA N(6)-methyladenosine editing by CRISPR-Cas9 conjugates. *Nat Chem Biol*. 2019;15:865–871.

Investigative Ophthalmology & Visual Science